An essential role for insulin and IGF1 receptors in regulating sertoli cell proliferation, testis size, and FSH action in mice.

Jean-Luc Pitetti, Pierre Calvel, Céline Zimmermann, Béatrice Conne, Marilena D Papaioannou, Florence Aubry, Christopher R Cederroth, Françoise Urner, Betty Fumel, Michel Crausaz, et al.

An Essential Role for Insulin and IGF1 Receptors in Regulating Sertoli Cell Proliferation, Testis Size, and FSH Action in Mice

Jean-Luc Pitetti, Pierre Calvel, Céline Zimmermann, Béatrice Conne, Marilena D. Papaioannou, Florence Aubry, Christopher R. Cederroth, Françoise Urner, Betty Fumel, Michel Crausaz, Mylène Docquier, Pedro Luis Herrera, François Pralong, Marc Germond, Florian Guillou, Bernard Jégou, and Serge Nef

Department of Genetic Medicine and Development (J.-L.P., P.C., C.Z., B.C., M.D.P., C.R.C., P.L.H., S.N.), University of Geneva Medical School and Genomics Platform (M.D.), National Center of Competence in Research "Frontiers in Genetics," University of Geneva, 1211 Geneva 4, Switzerland; Department of Internal Medicine (F.P.), University Hospital, 1011 Lausanne, Fondation pour l'Andrologie, la Biologie et l'Endocrinologie de la Reproduction and Centre for Medically Assisted Procreation (F.U., M.C., M.G.), 1003 Lausanne, Switzerland; Unité Physiologie de la Reproduction et des Comportements (B.F., F.G.), Unité Mixte de Recherche 6175, Institut National de la Recherche Agronomique-Centre National de la Recherche Scientifique-Université de Tours-Haras Nationaux, 37380 Nouzilly, France; and Institut National de la Santé et de la Recherche Médicale (F.A., B.J.), U625, Université Rennes I, Institut Fédératif de Recherche 140, Groupe d'Etude sur la Reproduction chez l'Homme et le Mammifère, F-35042, Rennes, France

Testis size and sperm production are directly correlated to the total number of adult Sertoli cells (SCs). Although the establishment of an adequate number of SCs is crucial for future male fertility, the identification and characterization of the factors regulating SC survival, proliferation, and maturation remain incomplete. To investigate whether the IGF system is required for germ cell (GC) and SC development and function, we inactivated the insulin receptor (*Insr*), the IGF1 receptor (*Igf1r*), or both receptors specifically in the GC lineage or in SCs. Whereas ablation of insulin/IGF signaling appears dispensable for GCs and spermatogenesis, adult testes of mice lacking both *Insr* and *Igf1r* in SCs (SC-*Insr;Igf1r*) displayed a 75% reduction in testis size and daily sperm production as a result of a reduced proliferation rate of immature SCs during the late fetal and early neonatal testicular period. In addition, in vivo analyses revealed that FSH requires the insulin/IGF signaling pathway to mediate its proliferative effects on immature SCs. Collectively, these results emphasize the essential role played by growth factors of the insulin family in regulating the final number of SCs, testis size, and daily sperm output. They also indicate that the insulin/IGF signaling pathway is required for FSH-mediated SC proliferation. (*Molecular Endocrinology* 27: 814–827, 2013)

Spermatogenesis refers to a complex differentiation process by which diploid spermatogonial stem cells develop into mature haploid spermatozoa. In the adult, Sertoli cells (SCs), the only somatic constituents of the seminiferous epithelium, are in direct physical association with all types of germ cells (GCs) and are mainly commit-

ISSN Print 0888-8809 ISSN Online 1944-9917
Printed in U.S.A.

Received August 6, 2012. Accepted March 14, 2013.
First Published Online March 21, 2013

Abbreviations: CASA, computer-assisted sperm analysis; E, embryonic day; FSHR, FSH receptor; GC, germ cell; GFP, green fluorescent protein; hCG, human chorionic gonadotropin; H&E, hematoxylin and eosin; 3β-HSD, 3β-hydroxysteroid dehydrogenase; IF, immunofluorescence; IGF1R, type I insulin-like growth factor receptor; IHC, immunohistochemistry; INSR, insulin receptor; LC, Leydig cell; MAPK, mitogen-activated protein kinase; P, postnatal day; PFA, paraformaldehyde; PI, propidium iodide; PI3K, phosphatidylinositol 3-kinase; PMC, peritubular myoid cell; PTU, 6-propyl-2-thiouracil; q, quantitative; SC, Sertoli cell; SMA, smooth muscle actin; TUNEL, terminal deoxynucleotidyl transferase dUTP nick-end labeling.

ted to sustain spermatogenesis. In particular, SCs provide GCs with a structural support and a preserved environment with the blood-testis barrier, assist their movement toward the seminiferous epithelium lumen and sustain their development through their secretory products (for reviews, see Refs. 1 and 2). Notably, individual SCs can only support a finite number of GCs. Therefore, the final testis size, the number of GCs in the adult testis, and sperm output are directly linked to the total number of SCs (3). It has been well established that the SC proliferation window in mice occurs during late fetal and early neonatal testicular development and the final adult number is reached by postnatal day (P) 15 (4, 5). This creates a stable, nondividing SC population that matures and progressively acquires the ability to sustain GC development (reviewed in Refs. 1 and 6).

Deciphering the factors that regulate the establishment of an adequate population of mature SCs and thus testis size remains one of the most critical questions in testicular biology. FSH is considered one of the major endocrine hormones regulating SC proliferation, with no synergistic or additive effect from androgens (3, 4, 7, 8). The influence of several other paracrine factors and systemic hormones (eg, thyroid hormones) in this process has also been described (9–16).

Insulin and its related growth factors IGF1 and IGF2 can modulate a variety of cellular activities including cell survival, stimulation of cell proliferation, differentiation, and metabolism (17, 18). The physiological effects of these factors are mediated through activation of 2 tyrosine kinase receptors: the insulin receptor (INSR) and the type I insulin-like growth factor receptor (IGF1R). Insulin and IGF1 bind primarily to INSR and IGF1R, respectively, whereas IGF2 binds, with somewhat similar affinities, to both receptors (19–21). Upon activation, INSR and IGF1R phosphorylate common substrates that activate a network of downstream effectors, including the phosphatidylinositol 3-kinase (PI3K) and the mitogen-activated protein kinase (MAPK) pathways, which are both associated with proliferation, differentiation, and cell survival (22, 23).

Several reports have shown that IGF1 regulates important testicular functions such as testosterone production by Leydig cells (LCs) (24). Unfortunately, little is known about the local actions that the insulin-like family of growth factors exert on GCs and SCs in vivo, because the constitutive invalidation of their cognate receptors systematically leads to perinatal lethality. To overcome these difficulties, we took advantage of the site specific Cre-lox recombination system to delete *Insr* and/or *Igf1r* specifically in SCs or the GC lineage during testicular development. By this means, we were able to demonstrate that the insulin/IGF growth factor family is an essential component of the endocrine and paracrine network that regulates testis growth and sperm production in mammals.

Materials and Methods

Animals

Insr^{flox} (*Insr*$^{fx/fx}$), Igf1r^{flox} (*Igf1r*$^{fx/fx}$), and MisCre (*Amh:Cre*) mice were provided by R. Kahn (Boston, Massachusetts), A. Efstratiadis (New York, New York), and F. Guillou (Tours, France), respectively, and were genotyped at weaning (P21) from tail biopsies by classic PCR as described previously (25–27). To analyze all different allelic inactivations, female mice carrying both *Insr* and *Igf1r* floxed alleles (*Insr*$^{fx/fx}$;*Igf1r*$^{fx/fx}$) were crossed with transgenic males expressing Cre-recombinase under the control of the *Mis* promoter to generate 50% *Insr*$^{fx/wt}$;*Igf1r*$^{fx/wt}$, and 50% *Insr*$^{fx/wt}$;*Igf1r*$^{fx/wt}$;*Amh:Cre* mice. These animals were subsequently intercrossed to generate Sertoli-specific deletions of *Insr* (*Insr*$^{fx/fx}$;*Amh:Cre*), *Igf1r* (*Igf1r*$^{fx/fx}$;*Amh:Cre*), or both *Insr* and *Igf1r* (*Insr*$^{fx/fx}$;*Igf1r*$^{fx/fx}$;*Amh:Cre*) as well as control animals (*Insr*$^{fx/fx}$;*Igf1r*$^{fx/fx}$ or *Insr*$^{fx/wt}$;*Igf1r*$^{fx/wt}$;*Amh:Cre)*. Selective inactivation of *Insr*, *Igf1r*, or *Insr;Igf1r* in male GCs was achieved using a similar strategy, taking advantage of 2 GC-specific Cre lines: a *Ngn3:Cre* transgene (P.L. Herrera, unpublished data) and a *Mvh:Cre* transgene (28). Both GC-specific Cre transgenic lines were genotyped by classic PCR using either Cre-recombinase–specific primers for the *Ngn3:Cre* transgene (20973, 5′-CCTGTTTTGCACGTTCACCG-3′; 20974, 5′-ATGCTTCTGTCCGTTTGCCG-3′) or a set of primers specific for the *Mvh;Cre* transgene as described previously (28). Animals were housed and cared for according to the ethical guidelines of the Direction Générale de la Santé of the Canton de Genève (experimentation ID: 1061/3430/1).

Fertility tests and sperm analysis

Mice lacking mice lacking *Insr, Igf1r*, and both in SCs (SC-*Insr*, SC-*Igf1r*, and SC-*Insr;Igf1r*, respectively) (n = 3–4) or control *Insr*$^{fx/fx}$;*Igf1r*$^{fx/fx}$ males were each bred with 2 6-week-old wild-type C57BL/6 female mice for a period of 6 months. Number of litters and pups per litter were systematically recorded. The epididymal sperm count was performed with sperm extracted from the caudal epididymis and ductus deferens of adult (P180) male mice and was analyzed for its concentration and viability as described previously (29–31). The testicular sperm count was evaluated from testis by enumeration of homogenization-resistant spermatid and spermatozoa nuclei using phase-contrast microscopy as described previously (32). In short, adult testis (P180) from 6 controls and 6 SC-*Insr;Igf1r* double-mutant mice were decapsulated and homogenized in a blender for 45 seconds in 6 and 3 mL of H_2O, respectively. After 2 rounds of sonication (12 kHz), an aliquot of the cell suspension was loaded on a Malassez hemocytometer and counted in duplicate.

Sperm motility

For each individual mouse, epididymal sperm were diluted in 1 mL of M2 medium just before analysis. Then 5 μl of the sperm suspension was deposited in a 20-μm-deep counting chamber

(Leja Products, Nieuw-Vennep, The Netherlands) and submitted to computer-assisted sperm analysis (CASA) (SCA system; Microptic SL, Barcelona, Spain). Five to 10 video sequences were recorded (25 frames/s) at 37°C using a negative phase-contrast ×10 objective. The sperm motility parameters examined in this study were curvilinear velocity (VCL; micrometers per second), straight-line velocity (VSL; micrometers per second), average path velocity (VAP; micrometers per second), amplitude of lateral head displacement (ALH; micrometers), beat-cross frequency (BCF; Hertz), linearity (LIN = VSL/VCL; percent), straightness (STR = VSL/VAP; percent), and wobble (WOB = VAP/VCL; percent). Motility was categorized as nonprogressive (VAP < 15 μm/s), slow progressive (VAP $> 15 <$ 45 μm/s), or fast progressive (VAP > 45 μm/s), as indicated by the manufacturer's instructions. The number of sperm present in the initial 1-mL suspension was calculated by the CASA system (10^6 sperm cells/mL).

Histology and immunohistochemistry (IHC)

Testes and epididymides were fixed overnight either in 4% paraformaldehyde (PFA) or in Bouin fixative and embedded in paraffin. Sections (5-μm) were stained with hematoxylin and eosin (H&E) or processed for IHC. For IHC analysis, PFA-fixed sections were incubated overnight at 4°C with the following antibodies: anti-INSR (1:100, sc-711; Santa Cruz Biotechnology, Santa Cruz, California), anti-IGF1R (1:50, sc-712; Santa Cruz Biotechnology); anti-GATA4 (1:50, sc-9053; Santa-Cruz Biotechnology), anti-$p27^{Kip1}$ (1:100, K0082–3S; MBL, Nagoya, Japan), anti-ZO1 (1:250, 61-7300; Zymed, South San Francisco, California), anti-panAKT (1:200, ref. no. 9272; Cell Signaling Technology, Danvers Massachusetts), anti-phospho-AKT (1:250, ref. no. 9271; Cell Signaling Technology), anti-smooth muscle actin (SMA) (1:100; gift from C. Chaponnier, Department of Pathology and Immunology, University of Geneva, Geneva, Switzerland), anti-β galactosidase (1:500, ab9361; Abcam, Cambridge, Massachusetts), anti-MVH (1:1000; gift from Toshiaki Noce, Mitsubishi Kagaku of Life Sciences, Tokyo, Japan), and anti-3β-hydroxysteroid dehydrogenase (HSD) (1:500; gift from Ian Mason, Queen Margaret University, Edinburg, United Kingdom). For fluorescent staining, Alexa-conjugated secondary antibodies (Invitrogen, Carlsbad, California) were used for signal revelations, whereas for stable staining, signals were revealed with 3,3′-diaminobenzidine (Sigma-Aldrich, Buchs, St-callen, Switzerland). All images were obtained with a Axioskop microscope (Carl Zeiss, Jena Germany) and processed using AxioVision software.

Proliferation and apoptosis assays

The proliferation assay was performed with PFA-fixed sections double stained with either anti-GATA4 (1:50, sc-9053; Santa-Cruz Biotechnology) and anti-Ki-67 (1:100, no. 556003; BD Biosciences, San Jose, California) overnight at 4°C or anti-GATA4 combined with the Click-iT EdU cell proliferation assay (Invitrogen) as described previously (33). A minimum of 3 different animals per genotype and developmental stage were analyzed. For each testis, between 3 and 5 sections distant from one another by at least 60 μm were selected, and pictures of 5 different fields per section were taken. Values are expressed as the percentage of proliferating SCs counted in a given region. Apoptotic assays were performed by means of both a terminal deoxynucleotidyl transferase dUTP nick-end labeling (TUNEL) reaction using an In Situ Cell Death Kit (Roche Applied Science, Indianapolis, Indiana) and double IHC using anti-cleaved caspase 3 (1:200, no. 9961L; Cell Signaling Technology) and anti-GCNA1 (1:50; gift from Dr G.C. Enders, University of Kansas Medical Center, Kansas City, Kansas) to reveal the identity of TUNEL-positive cells. The percentage of apoptotic, TUNEL-positive cells within the seminiferous epithelium was expressed as the average number of apoptotic cells within 20 seminiferous tubules.

Testis morphometry

Thirty transverse sections of seminiferous tubules from 3 different animals per genotype were randomly selected to measure small diameters. Diameters were measured in seminiferous tubule sections that were round or close to being round. Morphometric analysis was performed on a BX51 Olympus microscope, and the image was captured using a JVC video camera. Analysis was performed using the software package CAST Grid (version 2.4.1, The Computer Assisted Stereological Toolbox; Olympus, Tokyo, Japan). To obtain the volume density of seminiferous tubules, the total number of tubules (round or near round) was scored for each histological section, and an average area of tubule was measured from at least 25 randomly selected tubules. To obtain a more precise measure of testis volume, shrinkage areas were excluded from the testis surface. Because the specific gravity of testis tissue was considered to be 1.0, the seminiferous tubule volume is determined as the product of the volume density and testis weight. The total length of seminiferous tubules (meters) was obtained by dividing seminiferous tubule volume by the squared radius of the tubule times the π value (34).

DNA content analysis by flow cytometry

For DNA content analysis, control and mutant testes were dissected out, and GCs were isolated and stained with the intercalating agent propidium iodide (PI) as described previously (62). In short, control and SC-*Insr;Igf1r* testes (n = 5) at P180 were dissected out and decapsulated to release the seminiferous tubules. The latter were incubated in collagenase type IV (Sigma-Aldrich) at 37°C for up to 5 minutes under rapid agitation. Dispersed tubules were allowed to settle down and were washed twice with PBS without Ca^{2+} and Mg^{2+} (Sigma-Aldrich) to remove the LCs and the peritubular myoid cells. Washed tubules were then incubated for 5 minutes in 0.5% trypsin EDTA (Gibco; Invitrogen) and RQ1/DNase (1 μg/μL; Promega, Madison, Wisconsin) at 37°C under agitation. A cell suspension was obtained by pipetting gently several times before addition of 10 μL of heat-inactivated fetal calf serum to block trypsin activity. To generate a single-cell suspension, PBS without Ca^{2+} and Mg^{2+} was added, and the preparation was filtered through a 40-μm nylon cell strainer (BD Falcon; BD Biosciences Discovery Labware, Bedford, Massachusetts). For nuclear analysis, GCs were rinsed and resuspended in 1 mL of cold PI stain (10 mM Tris, pH 8.0, 1 mM NaCl, 0.1% NP40, 50 μg/mL PI, and 10 μg/mL RNase A), vortexed for 2 to 3 seconds, and incubated on ice for 10 minutes to both lyse the plasma membrane and stain nuclear DNA. DNA content was assessed using a FACSCalibur II (BD Biosciences).

Isolation of total RNAs and proteins from purified *Sox9:GFP*-positive SCs

Ir$^{fx/fx}$*;Igf1r*$^{fx/fx}$*;Mis:Cre* and control mice were bred with *Sox9:EGFP* knock-in mice to specifically label and sort SCs at embryonic day (E) 15.5, E17.5, P0, P5, P10, P15, and P60 (35). The introduction of an IRES-EGFP cassette into the 3′-untranslated region of the *Sox9* gene does not affect *Sox9* function because both heterozygous and homozygous animals are viable and fertile in contrast with *Sox9* null heterozygous mice (36). At relevant stages, control and SC-*Insr;Igf1r* male pups homozygous for *Sox9:EGFP* were killed (n = 5–10). Green fluorescent protein (GFP)-positive testes were decapsulated and incubated for 10 minutes in 0.5% trypsin EDTA and RQ1/DNase (4 mg/mL) at 37°C. To ensure complete cellular dissociation, an additive digestive step was performed by incubating the cell clusters in a solution/cocktail of collagenase (10 mg/mL), hyaluronidase (20 mg/mL), and DNase (4 mg/mL). To generate a single-cell suspension, PBS without Ca^{2+} and Mg^{2+} was added, and the preparation was filtered through a 40-μm nylon cell strainer (BD Falcon; BD Biosciences Discovery Labware). GFP^+ cells were sorted using a FACSVantage SE (BD Biosciences). For RNA extraction, GFP^+ or GFP^- cells were directly sorted in lysis buffer from an RNeasy kit and extracted using an RNeasy micro kit (Qiagen, Valencia, California), according to the manufacturer's protocol. RNA integrity and quantity were assessed using RNA 6000 picochips with a 2100 bioanalyzer (Agilent Technologies, Santa Clara, California).

Classic and quantitative (q) real-time PCR

Between 120 and 1 μg of total RNAs was reverse-transcribed with an Omniscript RT kit (Qiagen), according to the manufacturer's instructions, and 1/20 of the cDNA template was used as template for each PCR reaction. For regular RT-PCR amplification, a classic 30-cycle program was used as described previously (37). Real-time RT-PCR was performed on each sample in triplicate using an ABI 7900HT SDS system with Power SYBR Green PCR Master Mix (Applied Biosystems, Foster City, California). Data were analyzed using a comparative critical threshold (C_T) method with the amount of target gene normalized to the average of 3 endogenous control genes (*cyclophilin B*, *tubulin* α, and *tubulin* β). Normalized quantities were averaged for at least 3 replicates for each data point and are presented as the mean ± SD. The highest normalized relative quantity was arbitrarily designated as a value of 1.0. Fold changes were calculated from the quotient of means of these normalized quantities and are reported as the mean ± SEM. The primers used for classic and qRT-PCR are listed in Supplemental Table 1 published on The Endocrine Society's Journals Online web site at http://mend.endojournals.org.

Hemicastration, FSH injection, and 6-propyl-2-thiouracil (PTU) treatment

Newborn pups were either hemicastrated or sham-operated at birth under hypothermia-induced anesthesia (38). A small incision in the inguinal region was made, and the left testis was removed (39). Groups of control or hemicastrated pups were placed back with their mothers, and animals were killed at P60. For FSH treatment, newborn control and mutant pups were injected subcutaneously from birth (P0) to P10 with recombinant human FSH (Gonal-F; Merck Serono) dissolved in physiological solution (200 IU/kg in 0.9% NaCl) to induce SC proliferation as described previously (40). Pups were subjected to transient postnatal hypothyroidism by adding 0.1% PTU (Sigma-Aldrich) to the drinking water between birth and P25 as described previously (13). Then, pups were weaned, and tap water was given ad libitum thereafter to allow recovery to euthyroidism. Mice were killed at P60.

Human chorionic gonadotropin (hCG) stimulation and hormonal assay

To evaluate the basal and hCG-stimulated serum concentrations of testosterone, control and mutant animals were subjected to an ip injection of hCG (Chorulon, 15 IU/animal). Blood was collected from a retro-orbital sinus puncture before the injection to determine basal levels. Two hours later, by the time of killing, blood was collected by an intracardiac puncture. Sera were obtained by centrifugation (8000 rpm, 10 minutes) and conserved at −20°C until hormone assays were performed. FSH and LH levels were measured using an immunobeads Milliplex magnetic kit as recommended by the supplier (Millipore Corporation, Billerica, Massachusetts). Testosterone levels were evaluated by RIA using a Testosterone Double Antibody RIA Kit from MP Biomedicals (Solon, Ohio) and activin A using an Activin A Quantikine ELISA Kit from R&D Systems (Minneapolis, Minnesota).

Results

Expression profile of *Insr* and *Igf1r* and their ligands in SCs and male GCs

SCs provide a highly specialized environment crucial for spermatogonia renewal and GC progression into spermatogenesis. To determine in which cells IGFs might play a role in regulating testicular function, we analyzed by qRT-PCR the expression of the insulin-like family of growth factors and their receptors in purified GCs and SCs at P5. At this stage, seminiferous tubules are exclusively composed of proliferating, immature SCs (~84%) and primitive type A spermatogonia (~16%) (41). Taking advantage of a *Sox9-eGFP* knock-in mouse line that specifically labels SCs (35), we used fluorescence-activated cell sorting to isolate GFP^+ and GFP^- cell fractions from P5 testes. Both qRT-PCR and immunofluorescence (IF) analyses confirmed that the GFP^+ fraction was composed of highly purified SCs (95% purity), whereas the GFP^- fraction was composed mostly of GCs (~70%) and Leydig cells (~30%) (Supplemental Figure 1, A–C). We found that transcripts coding for the growth factors *Igf1* and *Igf2* were present at levels ~10-fold higher in the spermatogonia-enriched GFP^- fraction than in the GFP^+ fraction (Figure 1A). In contrast, transcripts for *Insr* and *Igf1r* were present at similar levels in immature SCs and spermatogonia-enriched fractions. These expression profiles were confirmed by a large-scale transcriptional anal-

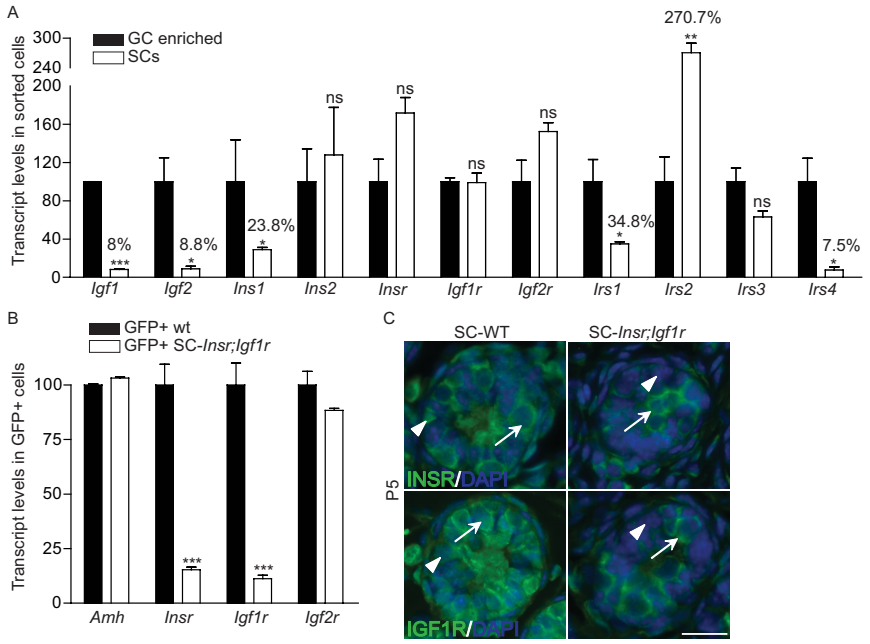

Figure 1. Expression profiles of *Insr*, *Igf1r*, and their ligands in purified gCs and SCs at P5. A, qRT-PCRs using as template total RNAs from purified populations of immature SCs (GFP$^+$ cells) and a GC-enriched fraction (GFP$^-$ cells) originating from P5 testis expressing the *Sox9-eGFP* allele. Note the high expression of *Igf1* and *Igf2* in male GCs, whereas transcripts coding for *Insr*, *Igf1r* are present both in the SCs and the enriched GC fraction. B, qRT-PCR using as template total RNAs from purified populations of immature SCs (GFP$^+$ cells) of both control *Sox9-eGFP* and mutant SC-*Insr;Igf1r;Sox9-eGFP* mice at P5. Note the massive reduction in transcripts coding for the *Insr* and *Igf1r* genes, whereas the expression of control genes such as *Amh* and *Igf2r* was not affected. Results are means ± SEM (n = 3/group). C, IF staining for INSR (green) or IGF1R (green) in both control and SC-*Insr;Igf1r* testes at P5. Note the absence of staining for the 2 receptors specifically in SCs. Arrowheads, SCs; arrows, GCs. Scale bar corresponds to 50 μm. DAPI, 4′,6′-diamidino-2-phenylindole.

ysis from a highly enriched population of mouse mature SCs, mitotic spermatogonia, meiotic spermatocytes, and postmeiotic round spermatids (42) (Supplemental Figure 1D). Overall, the robust expression of *Igf1* and *Igf2* in male GCs and the presence of transcripts coding for *Insr*, *Igf1r*, and the common effectors *Irs1* and *Irs2* in SCs and GCs suggest that the insulin-like family of growth factors exerts autocrine-paracrine actions within the seminiferous epithelium.

Massive reduction in SC number, testis size, and testicular sperm counts in mice lacking insulin/IGF signaling in developing SCs

To investigate the functional relevance of insulin/IGF signaling in both the GC and supporting cell lineages, we specifically deleted *Insr* (43), *Igf1r* (26), or both *Insr* and *Igf1r* either in the male germ line using a *Ngn3:Cre* transgenic line (44) or in SCs using an *Amh:Cre* transgene (27). Despite the fact that the *Ngn3:Cre* transgene was able to completely eliminate *Insr* and *Igf1r* in the male germ line, mice with a GC-specific deletion of *Insr*, *Igf1r*, or both *Insr* and *Igf1r* were viable and fertile (Supplemental Figure 2). All reproductive parameters were normal including typical testicular histology, testis size, and sperm production, indicating that the insulin/IGF signaling pathway is dispensable for differentiating male GCs throughout the meiotic and postmeiotic stages of spermatogenesis. We then examine the in vivo role of insulin/IGF signaling in SCs. For simplicity, SC-specific deletion of *Insr* (*Insr*$^{fx/fx}$;*AmhCre*), *Igf1r* (*Igf1r*$^{fx/fx}$;*AmhCre*), or both *Insr* and *Igf1r* (*Insr*$^{fx/fx}$;*Igf1r*$^{fx/fx}$;*AmhCre*) is abbreviated as SC-*Insr*, SC-*Igf1r*, and SC-*Insr;Igf1r*, respectively. Similarly, control mice bearing variable genotypes such as *Insr*$^{fx/fx}$, *Igf1r*$^{fx/fx}$, *Insr*$^{fx/fx}$;*Igf1r*$^{fx/fx}$, and *Insr*$^{wt/fx}$;*Igf1r*$^{wt/fx}$;*AmhCre* are abbreviated as wt because of the lack of phenotype (data not shown). *Amh*-driven *Cre* recombinase has been reported to efficiently delete floxed alleles specifically in SCs from E14.5 onward (27, 45). To assess the efficiency of the *Amh:Cre* transgene to eliminate specifically and completely both *Insr* and *Igf1r* transcripts in SCs, we crossed SC-*Insr;Igf1r* mutant mice with the *Sox9:EGFP* knock-in allele. We show by qRT-PCR that *Insr* and *Igf1r* transcripts were reduced by ~90% in the GFP$^+$ fractions of SC-*Insr*;*Igf1r* mutants (Figure 1B). This residual expression correlated well with the levels of GC contamination found in these GFP$^+$ fractions, suggesting that we achieved an efficient and specific ablation of both receptors in SCs. These results were confirmed by IF, showing that signals for both INSR and IGF1R were specifically absent in SCs of mutant testis at P5 (Figure 1C).

SC-*Insr*, SC-*Igf1r*, and SC-*Insr*;*Igf1r* mutants were all viable, grew to adulthood normally, and appeared to have normal sexual behavior and normal internal and external genitalia compared with those for control littermates. At P180, testes lacking *Insr*, *Igf1r*, or both *Insr* and *Igf1r* in SCs displayed weight reductions of 13.6%, 34.6%, and 72.4%, respectively, compared with those of their control littermates (Figure 2, A–D and I, and Supplemental Table 2). Histological analysis of mutant testes revealed no gross histological alteration of the seminiferous epithelium, with the presence of GCs at all stages of spermatogenesis and spermiogenesis (Figure 2, E–H). In contrast, epididymal sperm concentrations in SC-*Igf1r* and SC-

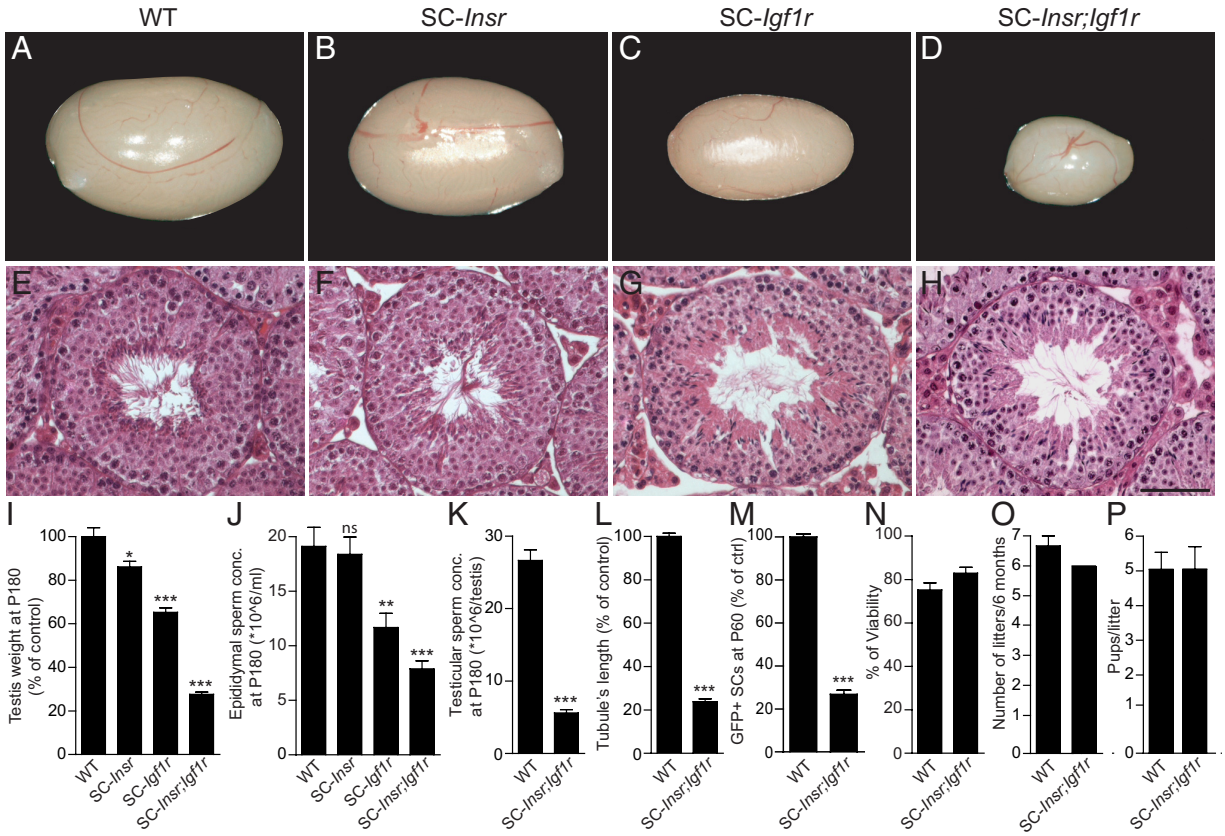

Figure 2. Reduced testis weight and sperm count in SC-*Insr*, SC-*Igf1r*, and SC-*Insr;Igf1r* testes at P180. Photomicrographs (A–D) and histological H&E sections (E–H) of wt (A and E), SC-*Insr* (B and F), SC-*Igf1r* (C and G), and SC-*Insr;Igf1r* (D and H) testes. Testis weights of SC-*Insr*, SC-*Igf1r*, and SC-*Insr;Igf1r* display 13.6%, 34.6%, and 72.4% reductions, respectively, compared with those for wt (I). Similarly, epididymal sperm concentrations were decreased by more than 38% and 58%, respectively, in SC-*Igf1r* and SC-*Insr;Igf1r* mutant animals (J). Testicular sperm concentration, a reflect of daily sperm production, was reduced by 72.4% in SC-*Insr;Igf1r* animals (K). Similarly, total seminiferous tubule's lengths (L) and GFP^+ SCs (M) were reduced by 75% in SC-*Insr;Igf1r* animals. In contrast, sperm viability assessed by ethidium monomer staining of the spermatozoa was not affected (N). A fertility assay performed with WT or SC-*Insr*, SC-*Igf1r*, and SC-*Insr;Igf1r* males mated with 2 C57BL/6 females over a period of 6 months (n = 3/genotype) did not reveal any reproductive defects because the number of litters (O) and the average pups per litter (P) were not affected. Values are expressed as means ± SEM. ns, not statistically significant; $*P < .05$ vs control; $**P < .01$ vs control; $***P < .001$ vs control. Scale bar in H corresponds to 50 μm.

Insr;*Igf1r* mutants were decreased by 38.85% and 58.71%, respectively, compared with those in control animals (Figure 2J and Supplemental Table 3). When the focus was exclusively on the double SC-*Insr*;*Igf1r* mutants, testicular sperm concentration, a reflection of daily sperm production, was also drastically reduced by 79% (Figure 2K). At this stage, neither the seminiferous epithelium architecture, the seminiferous tubule diameter, nor the SC number per tubule section was affected (Supplemental Figure 3, A–F). However, we observed a massive 75% reduction in tubule length (wt, 1.86 ± 0.1 m; SC-*Insr;Igf1r*, 0.42 ± 0.17 m; $P = .0002$) (Figure 2L), correlating well with a 74.3% reduction in the total number of SCs in SC-*Insr;Igf1r* mutant testes (Figure 2M).

Although sperm output was drastically reduced, sperm viability (Figure 2N) and sperm motility behavior were normal in SC-*Insr*, SC-*Igf1r*, and double SC-*Insr*;*Igf1r* mutant animals as measured by CASA (Supplemental Table 4). Because a reduction in sperm concentration could affect male reproductive function, we mated SC-*Insr*, SC-*Igf1r*, and double SC-*Insr*;*Igf1r* mutant males with 2 C57BL/6 female mice for a period of 6 months. Frequencies of parturition and litter size were not affected, indicating that loss of function of *Insr*, *Igf1r*, or both *Insr;Igf1r* in SCs does not impair reproductive ability despite oligospermia (Figure 2, O and P). Taken together, these results demonstrate that the massive reductions in testis size, tubule length, and sperm output in mutant animals is a consequence of a proportional reduction in the number of SCs.

Reduced SC proliferation in SC-*Insr;Igf1r* mice during late fetal and early neonatal testicular development

The establishment of an adequate number of SCs in the adult testis depends on the duration of the proliferative phase and the rate of division. We took advantage of the

Sox9;EGFP knock-in allele described previously to evaluate the progression in testis weight and SC numbers in both wt and SC-*Insr;Igf1r* mutant testes during late fetal and early neonatal testicular development. Whereas the first abnormalities in terms of testis weight appeared at P5 (Figure 3A), we observed a progressive and cumulative reduction of SC number in mutant animals during the late fetal and early neonatal stages of development (Figure 3B). At E17.5, about 3 to 4 days after the onset of *Amh;Cre* transgene expression, we already noticed a 40% reduction in SC number. This deficit in SCs worsened at later stages, reaching 43% at P0, 60% at P5, 67% at P15, and finally 74.3% at P60 (Figure 2M). A more refined analysis revealed that the daily rate of increase in SC number was primarily affected around E17.5 (−54%) and during the P0 to P5 period (−38%) (Figure 3C). This

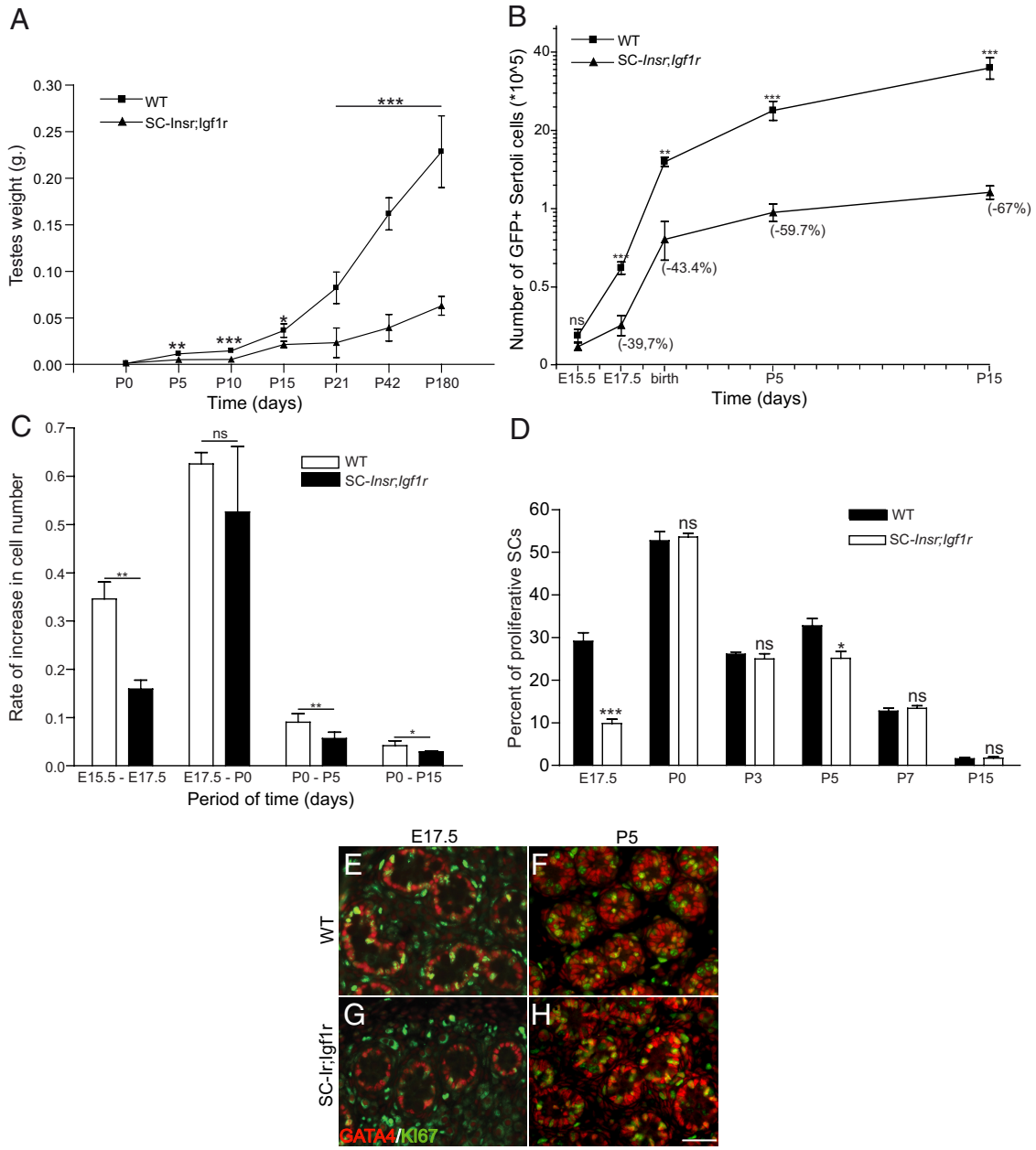

Figure 3. Reduced proliferation of immature SCs during the late fetal and early neonatal stage in SC-*Insr;Igf1r* mutants. A, Graph showing testis weight according to developmental stages (postnatal days). B, Graph depicting the number of GFP$^+$ SCs isolated from control (square) and SC-*Insr;Igf1r* (triangle) testes from E15 up to P60. In parentheses are the percentages of reduction at each relevant stages. C, Mean daily rate of increase in GFP$^+$ SCs during selected periods. D, Percentage of proliferating SCs at selected developmental stages. Note the significant reduction in the SC proliferative index during the E15.5 to E17.5 and P0 to P5 periods. Double IF using the SC marker GATA4 (red) and the proliferative marker Ki-67staining (green) is shown in both control (E and F) and SC-*Insr;Igf1r* mice (G and H) at E17.5 (E and G) and P5 (F and H). Values are expressed as means ± SEM. ns, not statistically significant; *$P < .05$ vs control; **$P < .01$ vs control; ***$P < .001$ vs control. Scale bar in H corresponds to 50 μm.

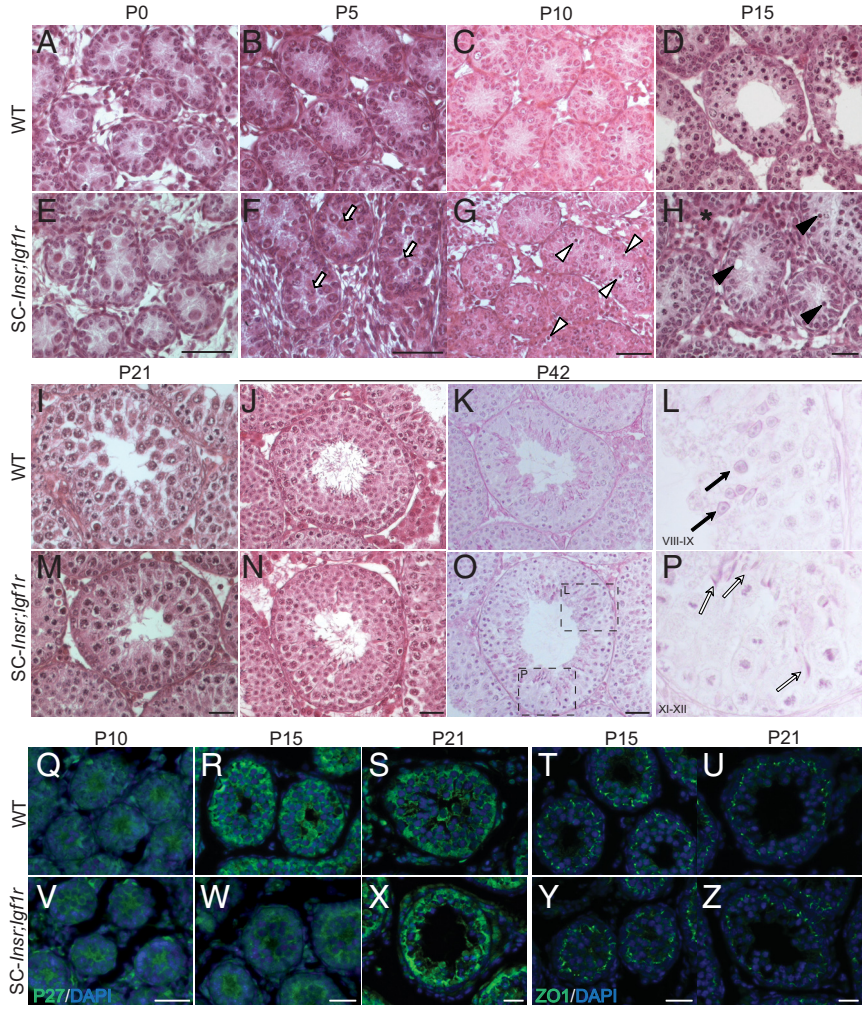

Figure 4. Seminiferous epithelium displays a transient delay in maturation between P0 and P42 in SC-*Insr;Igf1r* mutants. H&E staining from wt (A–D, I, and J) and SC-*Insr;Igf1r* (E–H, M, and N) mutant testes at P0 (A and E), P5 (B and F), P10 (C and G), P15 (D and H), P21 (I and M), and P42 (A, J, and N) reveals that mutant SCs display a delay in their maturation. Periodic acid-Schiff staining (K, L, O, and P) from wt (K) and SC-*Insr;Igf1r* (O and enlargement in L and P) mutant testes at P42 (A and E) showing a desynchronized progression of GCs as reflected by the simultaneous presence of spermatogenic stages VIII (L) and XII (M) within the same seminiferous tubule. IF against p27 and ZO1 confirm a partial delay of SC maturation (Q–Z). At P15, mutant testes display an absence of P27 staining (compare R with W). This delay is partial because the expression of ZO1 appears unaffected at P15 and P21 (T, U, Y, and Z). Scale bars correspond to 50 μm. DAPI, 4′,6′-diamidino-2-phenylindole.

dramatic reduction in testis size and total SC numbers during the late fetal/neonatal period led us to the assumption that the balance between cell proliferation and death had been perturbed in SCs lacking the insulin/IGF signaling pathway. As evidenced by double anti-GATA4/anti-Ki-67 IHC, SC proliferation rates were indeed reduced at 2 specific stages of development: by 66% at E17.5 and by 8% at P5 in SC-*Insr;Igf1r* testes compared with control testes (Figure 3, D–H). These results were confirmed by combining anti-GATA4 IF with the Click-iT EdU cell proliferation assay (Supplemental Figure 4). In contrast, apoptosis in SCs was unaffected (data not shown). These findings suggest that the striking testis size reduction observed in SC-*Insr;Igf1r* mice is a direct consequence of a reduced proliferation rate of immature SCs during the late fetal and early neonatal testicular period.

Transient delay in SC maturation and desynchronization of spermatogenesis in seminiferous tubules of SC-*Insr;Igf1r* testes

At E17.5 (data not shown) and birth (P0), double mutant testes displayed normal organization of the seminiferous epithelium and were histologically indistinguishable from controls (Figure 4, A and E). The first histological abnormalities appeared at P5 with spermatogonia being mislocalized in a central position instead of lying against the basement membrane (arrows in Figure 4F). We also observed 2- and 6-fold increases in the number of apoptotic GCs in P3 and P5 mutant testes compared with control testes (data not shown), correlating with the reduced number of SCs and the first histological abnormalities. At P10, we detected numerous pyknotic cells (white arrowheads) within testis cords and a hyperplasia of the interstitial tissue (Figure 4G). By P15, no lumen was observed in mutant seminiferous tubules, probably due to absence of seminiferous tubular fluid secretion (46) resulting from a delay in SC maturation (Figure 4H). In addition, several aspects of SC morphology suggested that these cells had remained in an immature state, because the nucleus did not reach a normal peripheral localization and strongly differed from the triangular shape characteristic of this developmental stage (Figure 4, D and H). We also observed vacuoles within tubules, a typical sign of GC sloughing. Delay in SC maturation was also investigated by immunohistochemical localization of protein markers associated with SC maturity such as p27, a marker of terminal differentiation, and Z01, a tight junction–associated protein essential for the blood-testis barrier (Figure 4, Q–Z). At P21, the few lumen that appeared late within the tubules

of SC-*Insr;Igf1r* testes displayed a smaller diameter than those found in control tubules (Figure 4M). However, spermatogenesis was normal in P21 mutant testes with the appearance of the first round spermatids. Finally, at P42, the first wave of GC meiosis was normally achieved in both control and double mutant testes, and all stages of differentiating GCs were present within the seminiferous tubules. Interestingly, we noticed that the seminiferous epithelium cycle is desynchronized in some SC-*Insr;Igf1r* seminiferous tubes, with individual sections having atypical GC associations containing step 1 round spermatids (black arrow) with step 8 elongated spermatids (white arrow) (Figure 4, L–P). These kinds of discrepancies were not observed in P180 mutant testis, indicating a transitory alteration of GC differentiation (Supplemental Figure 5). These data show that SC maturation is delayed in SC-*Insr;Igf1r* testes, resulting in a desynchronized progression of GCs during the first wave of spermatogenesis.

Morphology and function of Leydig cells and peritubular myoid cells were not affected in SC-*Insr;Igf1r* mutant testes

In addition to regulating spermatogenesis, SCs are also required to promote differentiation of both peritubular myoid cells (PMCs) and LCs (47). To investigate to what extent the numbers of PMCs and LCs were affected in SC-*Insr;Igf1r,* we performed IF assays using specific markers for both cell types. Using an antibody for SMA, we found that PMCs were not affected in terms of morphology, number/tubule, and localization in mutant testis (Figure 5A, B, and E). These results imply that the total number of PMCs present in the mutant testis is reduced to the proportion of the remaining SCs/seminiferous tubules. Using an anti-3βHSD to evaluate LC population, we found that the proportion of LCs present in the interstitial compartment was slightly increased in mutant testes (68% vs 61% in control) (Figure 5, C, D, and F). LC function was also evaluated by assessing the plasma levels of testosterone before (basal) and 2 hours after an ip injection of hCG (stimulated level). Although androgen levels in the basal state were not significantly affected, increased testosterone production by hCG was not as high as that in control animals (3.03-fold in mutant vs 7.69-fold in control animals) (Figure 5G). Interestingly, LH and activin levels were not affected, whereas FSH levels were 2.5-fold higher in mutant animals than in control mice (Figure 5, H–J). Overall, these results show that total numbers of LCs and PMCs are reduced at levels proportional to the number of SCs present in mutant testes. However, LC endocrine function was not significantly affected because basal testosterone levels were

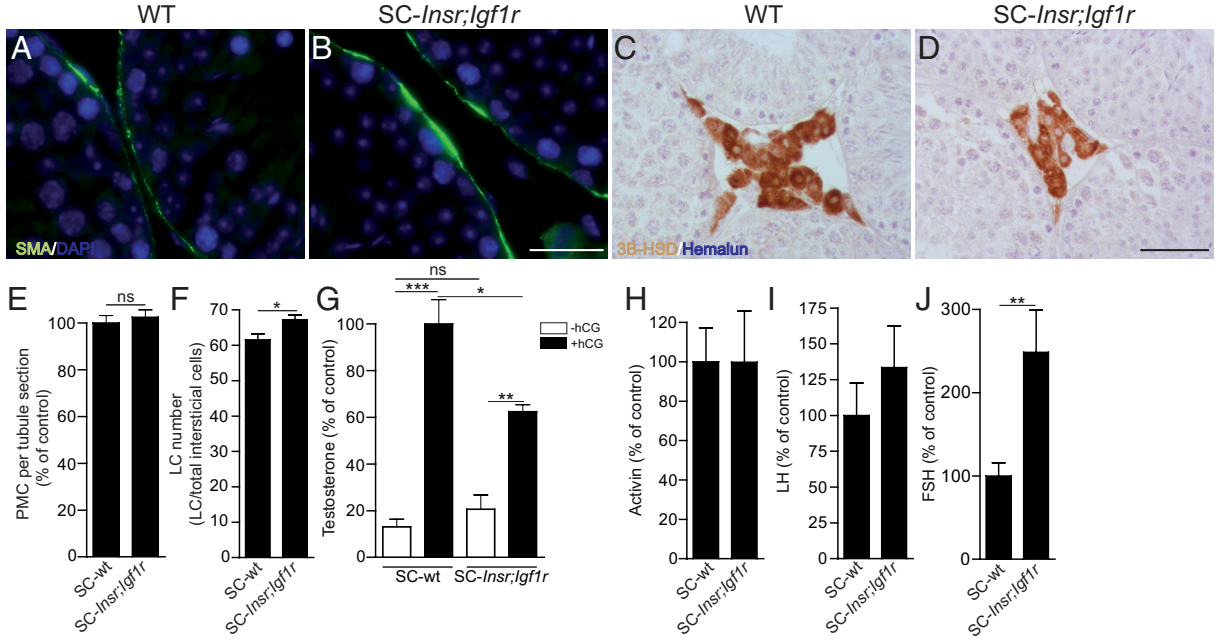

Figure 5. Both the morphology and function of LCs and PMCs were not affected in SC-*Insr;Igf1r* mutant testes. IF for SMA (A and B) and 3β-HSD (C and D) in both control (A and C) and SC-*Insr;Igf1r* (B and D) testes at P60 revealed that peritubular myoid cells (PMC) were not affected in terms of morphology or number/tubule (E), whereas the density of LCs in the interstitial compartment shows a slight increase in mutant testes (68% vs 61% in wt) (F). Plasma levels of FSH, LH, activin, and testosterone were evaluated in both control and mutant individuals (G–J). Basal testosterone (G), activin (H), and LH (I) levels were not affected, whereas testosterone levels under hCG stimulation were increased by 7.7- and 3-fold in control and SC-*Insr;Igf1r* individuals (G). FSH levels are 2.5-fold higher in the serum of in SC-*Insr;Igf1r* mutant animals (J). Values are expressed as means ± SEM. ns, not statistically significant; *$P < .05$ vs control; **$P < .01$ vs control; ***$P < .001$ vs control. Scale bars in B and D correspond to 50 μm. DAPI, 4′,6′-diamidino-2-phenylindole.

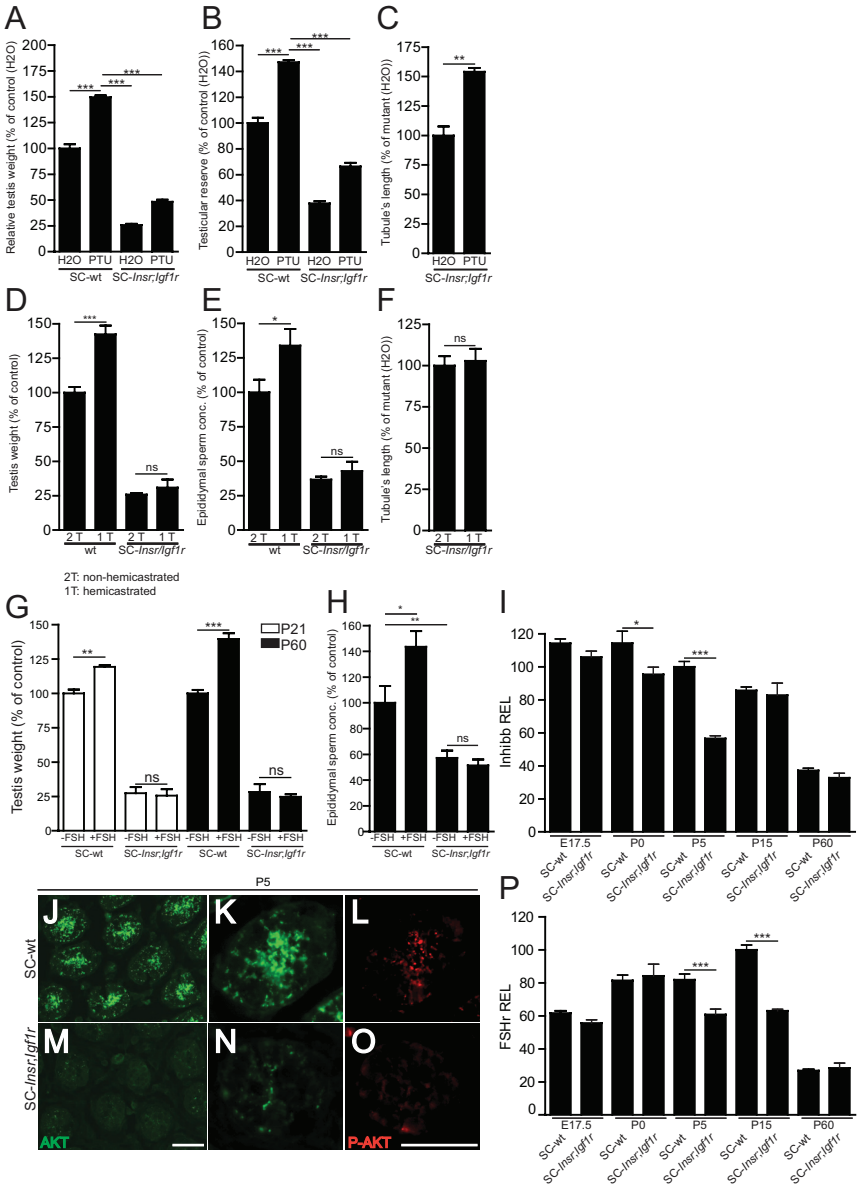

Figure 6. FSH action but not thyroid hormones requires insulin/IGF signaling to regulate SC proliferation and testis growth. Relative testis weight (A, D, and G), testicular reserve (B), epididymal reserve (E and H), and seminiferous tubule length (C and F) from control (wt) and SC-*Insr;Igf1r* mutant animals at P60 exposed postnatally to 0.1% PTU (A–C) or neonatally hemicastrated (D–F) or FSH treated between P0 and P10 (G and H). qRT-PCRs performed on cDNAs of *Sox9:GFP*$^{+}$ sorted SCs isolated by fluorescence-activated cell sorting at E17.5, P0, P5, P15, and P60 show a significant decrease in transcripts coding for both *Fshr* (P) and *inhibin* β (I) at P5 in SC-*Insr;Igf1r* mutant animals. IF staining against pan-AKT (J, K, M, and N) and phospho-AKT (L and O) at P5 in both control (J–L) and mutant animals (M–O). Note the drastic reduction of AKT and phospho-AKT signals in mutant compared with wt individuals. Values are expressed as means ± SEM. ns, not statistically significant; $*P < .05$ vs control; $**P < .01$ vs control; $***P < .001$ vs control. Scale bars in M and O correspond to 50 μm.

comparable and high enough to sustain normal spermatogenesis in mutant individuals.

Insulin/IGF signaling acts independently of thyroid hormones but is essential for FSH-mediated SC proliferation

The establishment of an adequate number of SCs in the adult testis depends on the duration of the proliferative phase and the rate of division. In mice, SCs proliferate from E12.5 through P10 (13), and both thyroid hormones and FSH are critical primary regulators of neonatal SC proliferation and functional maturation. The massive reduction in the total number of SCs in mutant testes (ie, 74%) raises the possibility that the insulin/IGF signaling pathway may be required either for T3 or FSH action on neonatal SC proliferation and maturation.

To study the potential interaction between T3 and the insulin/IGF signaling pathway, we induced transient hypothyroidism during early postnatal development by adding the goitrogen PTU (0.1%) to the water from birth to P25 either in wt or SC-*Insr;Igf1r* mutant males (Figure 6, A–C). In P60 wt animals exposed to PTU, the relative testis weight and testicular reserves were both substantially increased by 150% and 149%, respectively, as reported previously (13). Interestingly, in SC-*Insr;Igf1r* mutant mice, we observed a similar increase in relative testis weight and testicular sperm reserve after neonatal PTU treatment. This increase in testis weight and function was accompanied by a 154% increase in seminiferous tubule length, indicating that hypothyroidism increases SC number in the absence of the insulin/IGF signaling pathway. These findings reveal that T3 and insulin/IGFs act independently to modulate the number of SCs through different pathways and mechanisms.

In parallel, we used a model of neonatal hemicastration (38) to investigate the potential interaction between FSH and the insulin/IGF signaling pathway. Neonatal removal of a single gonad results in a significant increase in serum FSH concentration and a subsequent increase in the number of SCs as well as the size and the sperm production from the remaining testis (38, 39). Whereas testis size and epididymal sperm counts were increased by 142% and 134%, respectively, in hemicas-

trated control males, no effects on testicular function were observed in hemicastrated SC-*Insr;Igf1r* mutant mice. More precisely, testis weight, epididymal sperm count, and seminiferous tubule length were not affected by hemicastration and the subsequent increase in FSH levels in SC-*Insr;Igf1r* mutant mice (Figure 6, D–F). To confirm the key role played by the insulin/IGF signaling pathway in mediating FSH proliferative action on immature SCs, we treated newborn control and SC-*Insr;Igf1r* mutant mice between birth (P0) and P10 with recombinant human FSH at a concentration known to promote SC proliferation and testicular growth in rats (40). As expected, we found that testis size was significantly increased by 20% and 40% in control animals at P21 and P60, respectively. At P60, sperm output was also increased by 43% in controls (Figure 6H). In contrast, neither testis weight nor epididymal sperm counts were affected by FSH treatment in SC-*Insr;Igf1r* mutants compared with those in controls (Figure 6, G and H). Overall, these results indicate unambiguously that neonatal action of FSH requires the insulin/IGF signaling pathway to mediate its proliferative effects on immature SCs.

Both *Fshr* gene expression profile and AKT activation were affected in SCs lacking tINSR and IGF1R

In mutant animals, high FSH levels (Figure 5J) coupled with the inability to respond to FSH (Figure 6, D–H) suggest that FSH signaling may be affected in immature SCs lacking insulin/IGF signaling. Using qRT-PCR, we found in mutant purified SCs that transcript levels coding for the FSH receptor (FSHR) were reduced both at P5 and P15 by 26% and 37%, respectively (Figure 6P). In a similar manner, we found that *inhibin B* expression was also reduced in purified mutant SCs specifically at P0 and P5 (Figure 6J). In contrast, the expression of housekeeping genes as well as *Amh* was not affected, suggesting a specific alteration (data not shown). The reduced FSHR expression observed in mutant SCs should have a negative impact on FSH action and explain in part the incapacity of SCs lacking insulin/IGF signaling to proliferate after hemicastration or FSH treatment during the neonatal period.

Next we examined the expression and activation of protein kinase B/AKT, a signaling molecule that is part of the PI3K/AKT pathways known to be activated by both FSH and/or IGFs exposure in SCs and granulosa cells (48, 49). In control testes, we found by IF that AKT and its phosphorylated form were present at high levels specifically at P5 in the center of the testis cords, a region that corresponds to the cytoplasm of SCs (Figure 6, J–L). In contrast, we observed that immature SCs of mutant testes at P5 were almost devoid of AKT signal (Figure 6, M–O), suggesting that the PI3K/AKT signaling pathway is not functional in immature SCs around P5.

Discussion

The major objectives of this study were to investigate the potential roles of the insulin-like family of growth factors on testis development and spermatogenesis. By deleting *Insr* and/or *Igf1r* either in GCs or in SCs, we provide in vivo evidence that the insulin receptor family is dispensable in the GC lineage but plays a major role in regulating immature SC proliferation and maturation and ultimately the total pool of adult SCs. Compared with single receptor mutant mice, we observed a more severe reduction in total SC number and testis size in mice lacking both *Insr* and *Igf1r*, revealing a novel concerted action of both INSR and IGF1R in testicular development. In addition, both in vivo and in vitro analyses revealed that FSH requires the insulin/IGF signaling pathway to mediate its proliferative effects on immature SCs. Our data reinforce the view that the local production of insulin/IGF growth factors is the major intratesticular signal regulating SC number, testis size, and sperm output in mammals.

Although several factors play a role in the proliferation and maturation of SCs (50), insulin/IGF signaling is likely to represent the major hormonal signal involved in the establishment of a normal-sized cohort of SCs. When the influence of known factors affecting SC numbers such as FSH, androgens, or thyroid hormones are compared, our data indicate that the insulin signaling pathway is quantitatively the most important pathway regulating the final pool of SCs. In mice lacking the FSH receptor specifically in SCs (FSHRKO), the reduction in testis weight and SC number was approximately 55% to 60% (7) compared with >70% for SC-*Insr*;*Igf1r* mice. Similarly, transient neonatal hyperthyroidism resulted in a 50% reduction in the final SC number at P23 due to direct suppression of SC proliferation while their maturation is promoted (51) In contrast, androgens do not appear to have a direct effect on SC proliferation. Although androgens were initially shown to regulate SC proliferation in androgen-resistant *tfm* mice (52), the pool of adult SCs was not affected in mice lacking the androgen receptor specifically in the SC (SCARKO) (7), indicating that the androgen-dependent regulation of SC number is an indirect effect of androgen on the SC.

Interconnected actions of both FSH and IGF1 in regulating SC proliferation and function

The insulin/IGF family of growth factors acts mainly through INSR and IGF1R and activates 2 major signaling

pathways, namely the extracellular signal–regulated kinase/MAPK pathway and the PI3K/AKT pathway, both of which are important mediators of proliferation and cell survival. Although the FSHR belongs to the superfamily of G protein–coupled receptors, both the MAPK and PI3K/AKT pathways are also activated upon FSH binding to its receptor (for review, see 53), suggesting that FSH and IGF actions may be intricately interconnected and coordinated in SCs.

First, it has been shown that FSH is capable of stimulating the secretion of IGF1 by immature SCs (54–56). In addition, FSH has been shown to amplify IGF1-mediated PI3K/AKT signaling in SCs. These results provide evidence that FSH interacts with the IGF pathways at different levels to stimulate the secretion of IGF1 by SCs and also enhances its effects on PI3K/AKT signaling (48). Our in vivo results demonstrate that both INSR and IGF1R are required for FSH-mediated SC proliferation. However, the precise mechanism explaining how the insulin/IGF signaling pathway is required for FSH action in immature SCs is only starting to be unraveled. IGFs could act at several levels by stimulating either the expression of the FSHR and/or the activation of downstream signaling pathways common to both IGFs and FSH. Our expression analysis revealed first that *Fshr* transcripts were reduced in purified SCs lacking insulin/IGF signaling but only at P5 and P15 and not at earlier stages (Figure 6P). This reduction may affect FSH action and explain in part the incapacity of mutant SCs to proliferate after hemicastration or FSH treatment. Second, we also found that both INSR and IGF1R are required for AKT expression and activation in SCs at P5 (Figure 6, J-O) suggesting that AKT mediates the synergistic effect of FSH and IGFs on SC proliferation. Similar interactions between the IGF system and FSH have been reported in granulosa cells. *Fshr* expression and mRNA stability are increased by IGF-1 treatment in rat granulosa cells (57). In addition, it has been recently reported that IGFIR activity is essential for FSH-induced phosphorylation of AKT (49). Rat granulosa cells treated with a IGF1R inhibitor abolished AKT activation by FSH and prevented expression of steroidogenic genes and estradiol production. Taken together, these results obtained in both granulosa cells and SCs suggest a crucial role for IGFs in mediating FSH action in the gonads.

Insulin/IGF signaling in SCs is not essential for spermatogenesis and sperm production

The major role of SCs in the adult testis is to support GCs and secrete factors that control the survival and progression of GCs through the sequential steps of spermatogenesis. Based on in vitro studies suggesting that IGF1 regulates several functions of the mature SC (48, 58), we would have expected that ablation of insulin/IGF signaling in adult SCs or GCs would cause detrimental consequences for sperm production and mouse fertility. Surprisingly, this was not the case. First, ablation of both *Insr* and *Igf1r* in the GC lineage did not reveal alterations in sperm production and fertility (see Supplemental Figure 2). Second, although conditional deletion of *Insr* and *Igf1r* in SCs reduced drastically the final number of SCs by decreasing the survival rate and delaying differentiation of immature SCs, the capacity of adult SCs to support spermatogenesis is only mildly affected. A precise assessment of spermatogenesis in SC-*Insr;Igf1r* mutant mice at P60 revealed a small but significant decrease in the efficiency of sperm production. Using flow cytometry of PI-labeled cells to evaluate the abundance of haploid (1n; spermatids and spermatozoa), diploid (2n; spermatogonia A and B), and tetraploid cells (4n; spermatocytes I) in P60 adult animals, we found a decrease in the proportion of haploid cells in SC-*Insr;Igf1r* mutant testes (Supplemental Figure 6, A–C). Interestingly, the expression of some Sertoli-specific genes such as *inhibin* α and *Steel (KitL)* was significantly higher in SC-*Insr;Igf1r* testes, whereas other transcripts coding for *Amh*, *Gata1*, *transferrin*, *Pem*, and *testin* were not affected (Supplemental Figure 6D). Because inhibin is known to be stimulated by FSH, we also assessed gonadotropin and androgen levels in SC-*Insr;Igf1r* mutant mice. Although plasma levels of LH and activin were unaffected, we observed a significant 2.5-fold increase in FSH levels of SC-*Insr;Igf1r* mutant mice (Figure 5, G–J). Importantly, we observed significant 7.7- and 3-fold increase in testosterone levels of control and SC-*Insr;Igf1r* mutant mice after hCG stimulation, indicating normal although blunted androgen production by Leydig cells. These findings indicate that growth factors of the insulin family are key to regulating the final number of SCs and testis size but dispensable for SCs to support the spermatogenic process.

Receptor contribution

Comparative analysis of mutant animals lacking *Insr*, *Igf1r*, or both *Insr* and *Igf1r* in SCs provided information concerning the relative degree of contribution and functional redundancy of each receptor in regulating SC number and testis size. Testes lacking *Insr* or *Igf1r* in SCs displayed weight reductions of 13.6% and 34.6%, respectively, indicating that the contribution of IGF1R is more important than INSR. In addition, the concomitant ablation of both receptors resulted in a much more severe reduction in testis weight (72.4%), implying an important redundancy and suggesting that INSR and IGF1R act in a synergistic manner to regulate SC number and testis size.

Taking into account both the ligand-binding affinities and the relative contribution of INSR and IGF1R to the phenotype, we can obtain some important information concerning the identity of the potential ligand(s) mediating SC survival in the developing testis. The affinity of insulin for IGF1R has been reported to be 500 to 1000 times lower than that of the IGFs (59). IGF2 binds to its cognate receptor (IGF1R) and also to one of the insulin receptor isoforms (IR-A), exhibiting an affinity that is ~30% that of insulin (21, 60). Finally, IGF1 binds IGF1R with up to 20-fold higher affinity than IGF2 (61). The robust expression of IGF1 and IGF2 in spermatogonia (see Figure 1 and Supplemental Figure 1) raises the hypothesis that GCs themselves may finely regulate the number of SCs and thus testis size and daily sperm output, through the secretion of growth factors promoting SC survival and maturation during postnatal testicular development. Clearly further investigations are required to test this hypothesis.

Acknowledgments

Address all correspondence and requests for reprints to: Serge Nef, Department of Genetic Medicine and Development, University of Geneva Medical School, 1, rue Michel-Servet, CH 1211 Geneva 4, Switzerland. E-mail: serge.nef@unige.ch.

This work was supported by National Centers of Competence in Research Frontiers in Genetics and by the Département de l'Instruction Publique of the State of Geneva.

Author contributions include the following: S.N. and J.-L.P conceived and designed the experiments. J.-L.P., P.C., C.Z., B.C., M.D.P., F.A., C.C., F.U., B.F., M.C., and M.D. performed the experiments. S.N., J.-L.P., and P.C. analyzed the data. P.L.H., F.P., M.G., F.G., and B.J. contributed reagents/materials/analysis tools. S.N., J.-L.P., and P.C. wrote the manuscript.

Disclosure Summary: The authors have nothing to disclose.

References

1. **Jégou B.** The Sertoli cell. *Baillieres Clin. Endocrinol. Metab*. 1992; 6:273–311.
2. **Mruk DD, Cheng CY.** Sertoli-Sertoli and Sertoli-germ cell interactions and their significance in germ cell movement in the seminiferous epithelium during spermatogenesis. *Endocr Rev*. 2004;25:747–806.
3. **Orth JM, Gunsalus GL, Lamperti AA.** Evidence from Sertoli cell-depleted rats indicates that spermatid number in adults depends on numbers of Sertoli cells produced during perinatal development. *Endocrinology*. 1988;122:787–794.
4. **Baker PJ, O'Shaughnessy PJ.** Role of gonadotrophins in regulating numbers of Leydig and Sertoli cells during fetal and postnatal development in mice. *Reproduction*. 2001;122:227–234.
5. **Vergouwen RP, Jacobs SG, Huiskamp R, Davids JA, de Rooij DG.** Proliferative activity of gonocytes, Sertoli cells and interstitial cells during testicular development in mice. *J Reprod Fertil*. 1991;93: 233–243.
6. **Sharpe RM, McKinnell C, Kivlin C, Fisher JS.** Proliferation and functional maturation of Sertoli cells, and their relevance to disorders of testis function in adulthood. *Reproduction*. 2003;125:769–784.
7. **Abel MH, Baker PJ, Charlton HM, et al.** Spermatogenesis and Sertoli cell activity in mice lacking Sertoli cell receptors for follicle-stimulating hormone and androgen. *Endocrinology*. 2008;149: 3279–3285.
8. **Marshall GR, Plant TM.** Puberty occurring either spontaneously or induced precociously in rhesus monkey (*Macaca mulatta*) is associated with a marked proliferation of Sertoli cells. *Biol Reprod*. 1996; 54:1192–1199.
9. **Bagheri-Fam S, Argentaro A, Svingen T, et al.** Defective survival of proliferating Sertoli cells and androgen receptor function in a mouse model of the ATR-X syndrome. *Hum Mol Genet*. 2011;20:2213–2224.
10. **Boitani C, Stefanini M, Fragale A, Morena AR.** Activin stimulates Sertoli cell proliferation in a defined period of rat testis development. *Endocrinology*. 1995;136:5438–5444.
11. **Hu J, Shima H, Nakagawa H.** Glial cell line-derived neurotropic factor stimulates Sertoli cell proliferation in the early postnatal period of rat testis development. *Endocrinology*. 1999;140:3416–3421.
12. **Jaillard C, Chatelain PG, Saez JM.** In vitro regulation of pig Sertoli cell growth and function: effects of fibroblast growth factor and somatomedin-C. *Biol Reprod*. 1987;37:665–674.
13. **Joyce KL, Porcelli J, Cooke PS.** Neonatal goitrogen treatment increases adult testis size and sperm production in the mouse. *J Androl*. 1993;14:448–455.
14. **Petersen C, Boitani C, Fröysa B, Soder O.** Transforming growth factor-α stimulates proliferation of rat Sertoli cells. *Mol Cell Endocrinol*. 2001;181:221–227.
15. **Petersen C, Boitani C, Fröysa B, Söder O.** Interleukin-1 is a potent growth factor for immature rat Sertoli cells. *Mol Cell Endocrinol*. 2002;186:37–47.
16. **Fumel B, Guerquin MJ, Livera G, et al.** Thyroid hormone limits postnatal Sertoli cell proliferation in vivo by activation of its α1 isoform receptor (TRα1) present in these cells and by regulation of Cdk4/JunD/cmyc mRNA levels in mice. Biol Reprod 2012;87:16, 1–9
17. **Efstratiadis A.** Genetics of mouse growth. *Int J Dev Biol*. 1998;42: 955–976.
18. **Nakae J, Kido Y, Accili D.** Distinct and overlapping functions of insulin and IGF-I receptors. *Endocr Rev*. 2001;22:818–835.
19. **Baker J, Liu JP, Robertson EJ, Efstratiadis A.** Role of insulin-like growth factors in embryonic and postnatal growth. *Cell*. 1993;75: 73–82.
20. **Liu JP, Baker J, Perkins AS, Robertson EJ, Efstratiadis A.** Mice carrying null mutations of the genes encoding insulin-like growth factor I (Igf-1) and type 1 IGF receptor (Igf1r). *Cell*. 1993;75:59–72.
21. **Louvi A, Accili D, Efstratiadis A.** Growth-promoting interaction of IGF-II with the insulin receptor during mouse embryonic development. *Dev Biol*. 1997;189:33–48.
22. **Avruch J.** Insulin signal transduction through protein kinase cascades. *Mol Cell Biochem*. 1998;182:31–48.
23. **Taniguchi CM, Emanuelli B, Kahn CR.** Critical nodes in signalling pathways: insights into insulin action. *Nat Rev Mol Cell Biol*. 2006; 7:85–96.
24. **Baker J, Hardy MP, Zhou J, et al.** Effects of an Igf1 gene null mutation on mouse reproduction. *Mol Endocrinol*. 1996;10:903–918.
25. **Brüning JC, Gautam D, Burks DJ, et al.** Role of brain insulin receptor in control of body weight and reproduction. *Science*. 2000; 289:2122–2125.

26. **Dietrich P, Dragatsis I, Xuan S, Zeitlin S, Efstratiadis A.** Conditional mutagenesis in mice with heat shock promoter-driven cre transgenes. *Mamm Genome*. 2000;11:196–205.
27. **Lécureuil C, Fontaine I, Crepieux P, Guillou F.** Sertoli and granulosa cell-specific Cre recombinase activity in transgenic mice. *Genesis*. 2002;33:114–118.
28. **Gallardo T, Shirley L, John GB, Castrillon DH.** Generation of a germ cell-specific mouse transgenic Cre line, *Vasa-Cre*. *Genesis*. 2007;45:413–417.
29. **Guerif F, Cadoret V, Plat M, et al.** Characterization of the fertility of Kit haplodeficient male mice. *Int J Androl*. 2002;25:358–368.
30. **Surace EI, Strickland A, Hess RA, Gutmann DH, Naughton CK.** Tslc1 (nectin-like molecule-2) is essential for spermatozoa motility and male fertility. *J Androl*. 2006;27:816–825.
31. **Touré A, Lhuillier P, Gossen JA, et al.** The testis anion transporter 1 (Slc26a8) is required for sperm terminal differentiation and male fertility in the mouse. *Hum Mol Genet*. 2007;16:1783–1793.
32. **Jégou B, Velez de la Calle JF, Bauché F.** Protective effect of medroxyprogesterone acetate plus testosterone against radiation-induced damage to the reproductive function of male rats and their offspring. *Proc Natl Acad Sci USA*. 1991;88:8710–8714.
33. **Salic A, Mitchison TJ.** A chemical method for fast and sensitive detection of DNA synthesis in vivo. *Proc Natl Acad Sci USA*. 2008; 105:2415–2420.
34. **França LR, Godinho CL.** Testis morphometry, seminiferous epithelium cycle length, and daily sperm production in domestic cats (*Felis catus*). *Biol Reprod*. 2003;68:1554–1561.
35. **Nel-Themaat L, Vadakkan TJ, Wang Y, Dickinson ME, Akiyama H, Behringer RR.** Morphometric analysis of testis cord formation in Sox9-EGFP mice. *Dev Dyn*. 2009;238:1100–1110.
36. **Bi W, Huang W, Whitworth DJ, et al.** Haploinsufficiency of Sox9 results in defective cartilage primordia and premature skeletal mineralization. *Proc Natl Acad Sci USA*. 2001;98:6698–6703.
37. **Nef S, Schaad O, Stallings NR, et al.** Gene expression during sex determination reveals a robust female genetic program at the onset of ovarian development. *Dev Biol*. 2005;287:361–377.
38. **Orth JM, Higginbotham CA, Salisbury RL.** Hemicastration causes and testosterone prevents enhanced uptake of [^{3}H] thymidine by Sertoli cells in testes of immature rats. *Biol Reprod*. 1984;30:263–270.
39. **Simorangkir DR, de Kretser DM, Wreford NG.** Increased numbers of Sertoli and germ cells in adult rat testes induced by synergistic action of transient neonatal hypothyroidism and neonatal hemicastration. *J Reprod Fertil*. 1995;104:207–213.
40. **Nurmio M, Kallio J, Adam M, Mayerhofer A, Toppari J, Jahnukainen K.** Peritubular myoid cells have a role in postnatal testicular growth. *Spermatogenesis*. 2012;2:79–87.
41. **Bellvé AR, Cavicchia JC, Millette CF, O'Brien DA, Bhatnagar YM, Dym M.** Spermatogenic cells of the prepuberal mouse. Isolation and morphological characterization. *J Cell Biol*. 1977;74:68–85.
42. **Chalmel F, Rolland AD, Niederhauser-Wiederkehr C, et al.** The conserved transcriptome in human and rodent male gametogenesis. *Proc Natl Acad Sci USA*. 2007;104:8346–8351.
43. **Brüning JC, Michael MD, Winnay JN, et al.** A muscle-specific insulin receptor knockout exhibits features of the metabolic syndrome of NIDDM without altering glucose tolerance. *Mol Cell*. 1998;2:559–569.
44. **Korhonen HM, Meikar O, Yadav RP, et al.** Dicer is required for haploid male germ cell differentiation in mice. *PLoS One*. 2011;6: e24821.
45. **Papaioannou MD, Pitetti JL, Ro S, et al.** Sertoli cell Dicer is essential for spermatogenesis in mice. *Dev Biol*. 2009;326:250–259.
46. **Rato L, Socorro S, Cavaco JE, Oliveira PF.** Tubular fluid secretion in the seminiferous epithelium: ion transporters and aquaporins in Sertoli cells. *J Membr Biol*. 2010;236:215–224.
47. **Yao HH, Whoriskey W, Capel B.** Desert Hedgehog/Patched 1 signaling specifies fetal Leydig cell fate in testis organogenesis. *Genes Dev*. 2002;16:1433–1440.
48. **Khan SA, Ndjountche L, Pratchard L, Spicer LJ, Davis JS.** Follicle-stimulating hormone amplifies insulin-like growth factor I-mediated activation of AKT/protein kinase B signaling in immature rat Sertoli cells. *Endocrinology*. 2002;143:2259–2267.
49. **Zhou P, Baumgarten SC, Wu Y, et al.** IGF-I signaling is essential for FSH stimulation of AKT and steroidogenic genes in granulosa cells. *Mol Endocrinol*. 2013;27:511–523.
50. **Mackay S, Smith RA.** Effects of growth factors on testicular morphogenesis. *Int Rev Cytol*. 2007;260:113–173.
51. **van Haaster LH, de Jong FH, Docter R, de Rooij DG.** High neonatal triiodothyronine levels reduce the period of Sertoli cell proliferation and accelerate tubular lumen formation in the rat testis, and increase serum inhibin levels. *Endocrinology*. 1993;133:755–760.
52. **Johnston H, Baker PJ, Abel M, et al.** Regulation of Sertoli cell number and activity by follicle-stimulating hormone and androgen during postnatal development in the mouse. *Endocrinology*. 2004; 145:318–329.
53. **Walker WH, Cheng J.** FSH and testosterone signaling in Sertoli cells. *Reproduction*. 2005;130:15–28.
54. **Cailleau J, Vermeire S, Verhoeven G.** Independent control of the production of insulin-like growth factor I and its binding protein by cultured testicular cells. *Mol Cell Endocrinol*. 1990;69:79–89.
55. **Chatelain P, Naville D, Avallet O, et al.** Paracrine and autocrine regulation of insulin-like growth factor I. *Acta Paediatr Scand Suppl*. 1991;372:92–95; discussion 96.
56. **Palmero S, Prati M, Barreca A, Minuto F, Giordano G, Fugassa E.** Thyroid hormone stimulates the production of insulin-like growth factor I (IGF-I) by immature rat Sertoli cells. *Mol Cell Endocrinol*. 1990;68:61–65.
57. **Minegishi T, Hirakawa T, Kishi H, et al.** A role of insulin-like growth factor I for follicle-stimulating hormone receptor expression in rat granulosa cells. *Biol Reprod*. 2000;62:325–333.
58. **Froment P, Vigier M, Nègre D, et al.** Inactivation of the IGF-I receptor gene in primary Sertoli cells highlights the autocrine effects of IGF-I. *J Endocrinol*. 2007;194:557–568.
59. **De Meyts P, Wallach B, Christoffersen CT, et al.** The insulin-like growth factor-I receptor. Structure, ligand-binding mechanism and signal transduction. *Horm Res*. 1994;42:152–169.
60. **Frasca F, Pandini G, Scalia P, et al.** Insulin receptor isoform A, a newly recognized, high-affinity insulin-like growth factor II receptor in fetal and cancer cells. *Mol Cell Biol*. 1999;19:3278–3288.
61. **Germain-Lee EL, Janicot M, Lammers R, Ullrich A, Casella SJ.** Expression of a type I insulin-like growth factor receptor with low affinity for insulin-like growth factor II. *Biochem J*. 1992;281(Pt 2):413–417.
62. **Cederroth CR, Zimmermann C, Beny JL, et al.** Potential detrimental effects of a phytoestrogen-rich diet on male fertility in mice. *Mol Cell Endocrinol*. 2010;321(2):152–160.